2023

Optical chip detecting ultrafast currents. — The carrier-envelope phase (CEP) is an important property of few-cycle laser pulses, allowing for light field control of electronic processes during laser- matter interactions. Thus, the measurement and control of CEP is essential for applications of few-cycle lasers. Currently, there is no robust method for measuring the non-trivial spatial CEP distribution of few-cycle laser pulses. In a paper published in Nature Communications journal [1] we demonstrated a compact on-chip, ambient-air, CEP scanning probe with 0.1 μm^3 resolution based on optical driving of CEP-sensitive ultrafast currents in a metal–dielectric heterostructure. We successfully applied the probe to obtain a 3D map of spatial changes of CEP in the vicinity of an oscillator beam focus with pulses as weak as 1 nJ, see Figure 1. We also demonstrated CEP control in the focal volume with a spatial light modulator so that arbitrary spatial CEP sculpting could be realized.

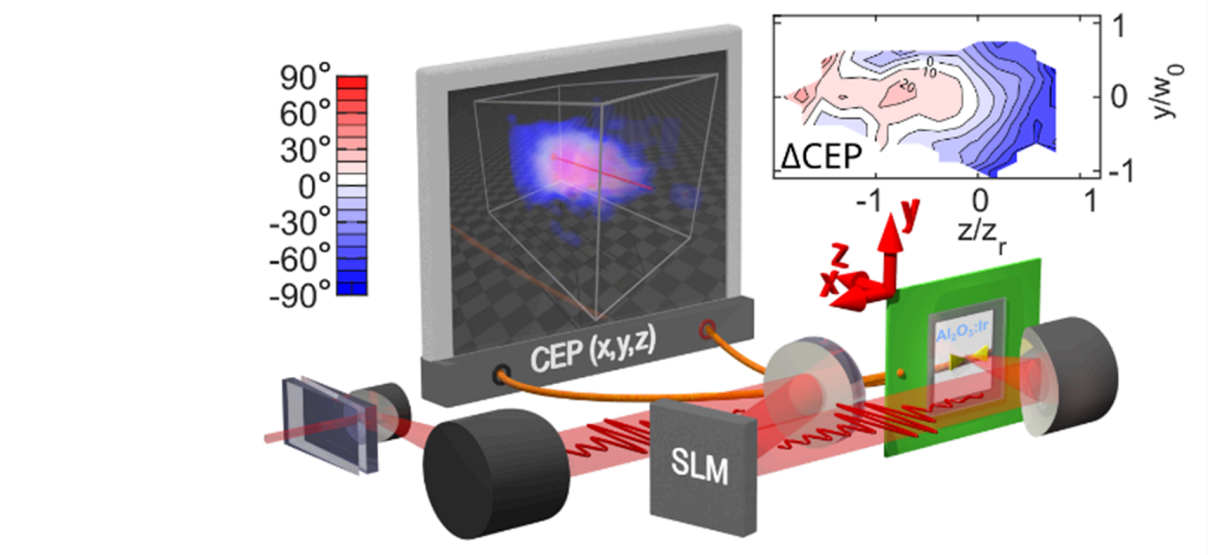

Figure 1. Mapping the CEP of laser pulses: An ultrashort pulse of laser light impinges on the probe and induces current that is proportional to the CEP property of the pulse. The probe is scanned within the focus, providing a 3D map of the CEP (colored 3D cloud, the inset shows a 2D cross-section).

Subcycle photoemission driven by ultrastrong terahertz pulses — The advent of intense terahertz (THz) sources opened a new era when the demonstration of the acceleration and manipulation of free electrons by THz pulses became within reach. THz-field-driven electron emission was predicted to be confined to a single burst due to the single-cycle waveform. In a paper published in Nature Communications journal [2] we demonstrated the confinement of single-cycle THz-waveform-driven electron emission to one of the two half cycles from a solid surface emitter. Either the leading or the trailing half cycle was active, controlled by reversing the field polarity. THz-driven single-burst surface electron emission sources, which do not rely on field-enhancement structures, will impact the development of THz- powered electron acceleration and manipulation devices, all-THz compact electron sources, THz waveguides and telecommunication, THz-field-based measurement techniques and solid-state devices.

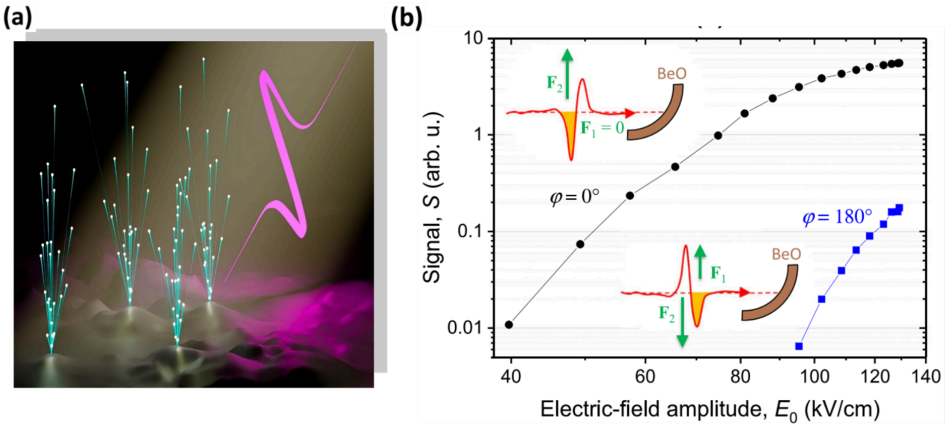

Figure 2. (a) An artistic idea of the one cycle THz-pulse-induced electron emission from a metal. (b) Experimental results demonstrating the switching effect of the asymmetric THz field on the electron emission. Flipping the field's polarity by changing the phase from ϕ = 0° (black) to ϕ = 180° (blue) leads to the photoemission signal turn-off, as only the into-material pointing crest of the field causes the emission. If the driving field's amplitude is brought to such a level that the field magnitude of the weaker crest approaches the magnitude of the stronger one of the lower amplitude, the electron signal emerges (blue squares).

References:

[1] DOI: 10.1038/s41467-023-40802-z

[2] DOI: 10.1038/s41467-023-42316-0

2022

Nonadiabatic tunneling. — Nonadiabatic nano-optical electron tunneling in the transition region between multiphoton-induced emission and adiabatic tunnel emission was explored experimentally in the near-field of plasmonic nanostructures (Fig. 1). We published the corresponding results in Nano Letters [1]. For Keldysh γ values between ~1.3 and ~2.2, measured photoemission spectra show strong-field recollision driven by the nanoscale near-field. At the same time, the photoemission yield shows an intensity scaling with a constant nonlinearity, which is characteristic for multiphoton-induced emission. Our observations in this transition region were well reproduced with the numerical solution of Schrödinger's equation, mimicking the nanoscale geometry of the field. This way, we determined the boundaries and nature of nonadiabatic tunneling photoemission, building on a key advantage of a nanoplasmonic system, namely, that high-field-driven recollision events and their signature in the photoemission spectrum can be observed more efficiently due to significant nanoplasmonic field enhancement factors. We also performed additional analysis of the ultrafast photoemission process [2].

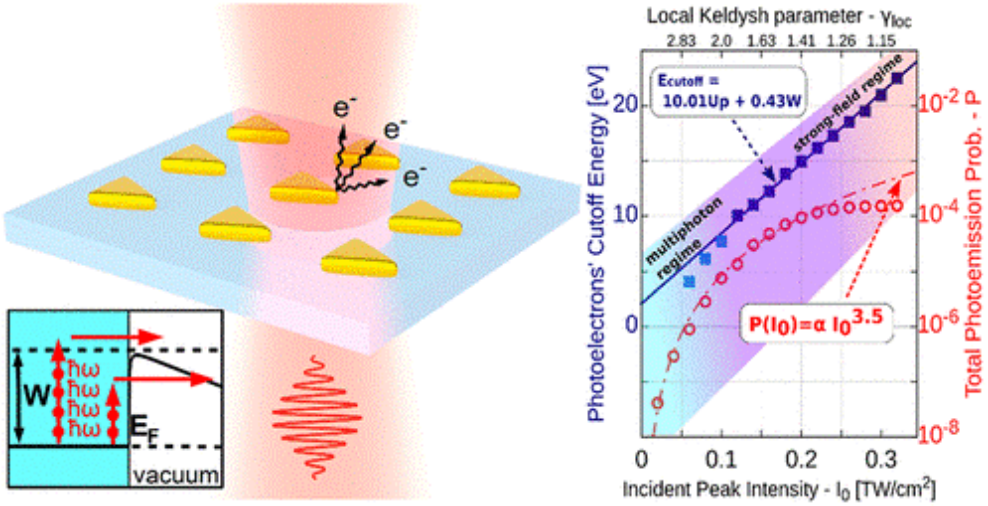

Figure 1. The scheme of the experiment and a simultaneous plot of the photoelectron yield and electrons spectral cutoff energies.

Hot electron science. — Non-thermal and thermal carrier populations in plasmonic systems raised significant interest in contemporary fundamental and applied physics. Although the theoretical description predicts not only the energies but also the location of the generated carriers, the experimental justification of these theories is still lacking. We demonstrated experimentally that upon the optical excitation of surface plasmon polaritons, a non-thermal electron population appears in the topmost domain of the plasmonic film directly coupled to the local fields (Fig. 2). We published the corresponding results in Nature Communications [3]. The applied all-optical method is based on spectroscopic ellipsometric determination of the dielectric function, allowing us to obtain in-depth information on surface plasmon induced changes of the directly related electron occupancies. The ultrahigh sensitivity of our method allows us to capture the signatures of changes induced by electron-electron scattering processes with ultrafast decay times. These experiments shed light on the build-up of plasmonic hot electron population in nanoscale media.

In addition, we demonstrated control possibilities of plasmonic fields with the help of mode-mixing by adjusting the polarization state of the excitation laser [4]. Finally, we investigated the formation of laser induced periodic surface structures in indium-tin-oxide (ITO) films [5].

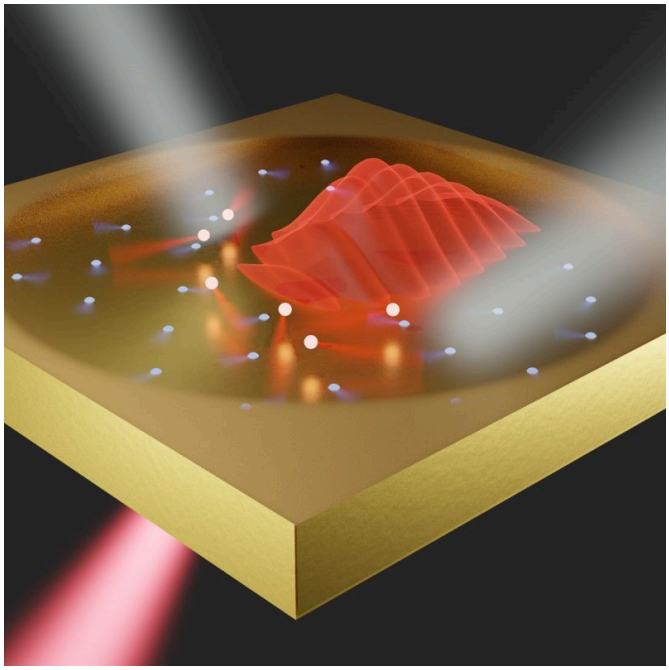

Figure 2. Illustration of hot electron generation and the corresponding near-fields in plasmonic thin films.

2020

Laser-induced currents in dielectrics — Future PHz electronic devices promise performing operations on few-femtosecond time-scales. They are based on the control of currents in materials induced by intense few-cycle laser pulses. Investigations of this control scheme have been based on complex, amplified laser systems, typically delivering mJ or sub-mJ-level laser pulses, limiting the achievable clock rate to the kHz regime. We demonstrated transient metalization and lightwave-driven current control with 300-pJ laser pulses at 80 MHz repetition rate in dielectric media (HfO_2 and fused silica), and the wide-bandgap semiconductor GaN, for the first time to our knowledge (Fig. 1). We determined the field strength dependence of optically-induced currents in these media. Supported by a theoretical model, we showed scaling behaviors that will be instrumental in the construction of PHz electronics devices.

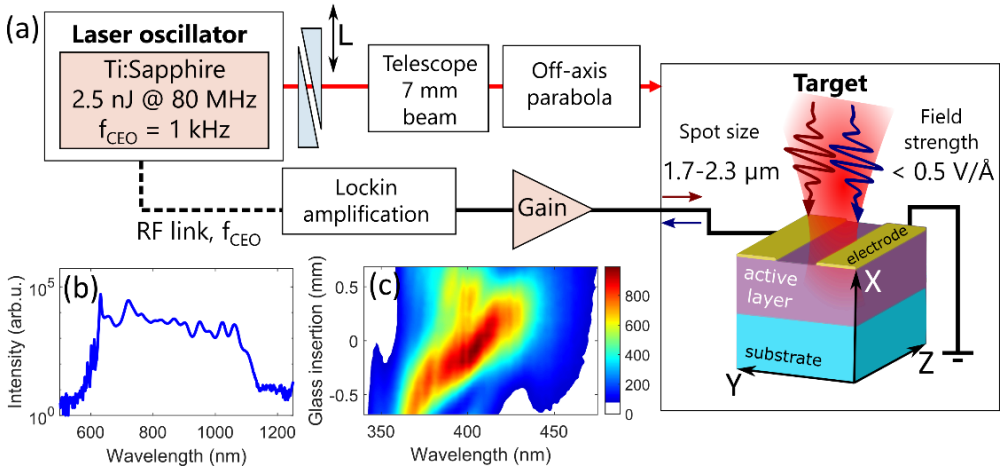

Figure 1. *(a) Scheme for laser-induced current control in dielectric media. (b) Spectrum of the ultrashort-pulse laser used. (c) Dipersion-scan pulse characterization of 5.5-fs laser pulses used for the experiments.*

Strong-field nano-optics — We published an important review paper in Rev. Mod. Phys., the world leading review journal in physics with the title "Storng-field nano-optics" on this emerging field of research [1].

We studied the evolution of femtosecond breakdown in lithographically produced plasmonic nanoparticles with increasing laser intensity [2]. Localized plasmons were generated with 40-fs laser pulses with up to 1.4×10^{12} W/cm^2 peak intensity. The damage morphology shows substantial variation with intensity, starting with the detachment of hot spots and stochastic nanoparticle removal, ranging to precise nanolithographic mapping of near-field distributions via ablation. The common feature of these phenomena is the central role played by the single plasmonic hot spot of the triangular nanoparticles used. We also derive a damage threshold value from stochastic damage trends on the arrays fostering the optimization of novel nanoarchitectures for nonlinear plasmonics and plasmonically enhanced high harmonic generation.
We studied how the collective effects of nanoparticles arranged in rectangular arrays influence their temporal plasmon response and field enhancement property [3]. By systematically changing the lattice constant for arrays containing identical metal nanorods, we experimentally demonstrate how grating induced effects affect the position and, more importantly, the broadening of extinction spectra. We correlated these effects with the achievable field enhancement and the temporal duration of plasmon transients and formulate criteria for the generation of enhanced few-cycle localized plasmon oscillations.

2019

Strong-field interactions and nano-optics experiments. — After establishing ultrafast plasmonic photoelectrons as versatile probes for nanoplasmonic near-fields (see e.g.), we extended this method to probe the evolution of plasmonic near-fields on few-femtosecond time-scales, representing the natural time-scale of the buildup and decay of collective electron oscillations by light. We performed time-resolved experiments with unprecedented resolution, the results of which are under analysis.

We also performed high order harmonics generation (HHG) experiments on noble gas cluster targets with different cluster sizes. The independently characterized cluster sources enabled experimental investigation of the recombination mechanism. HHG spectra were recorded for different backing pressures and gases (Ar, Xe) as a function of driver pulse ellipticity (Fig. 1). Since the ellipticity-dependent HHG decay is essentially the same for the different gas-pressure pairs, we can conclude that the recombination process is dominated by atom-to-itself recollisions irrespective of the cluster size and material .

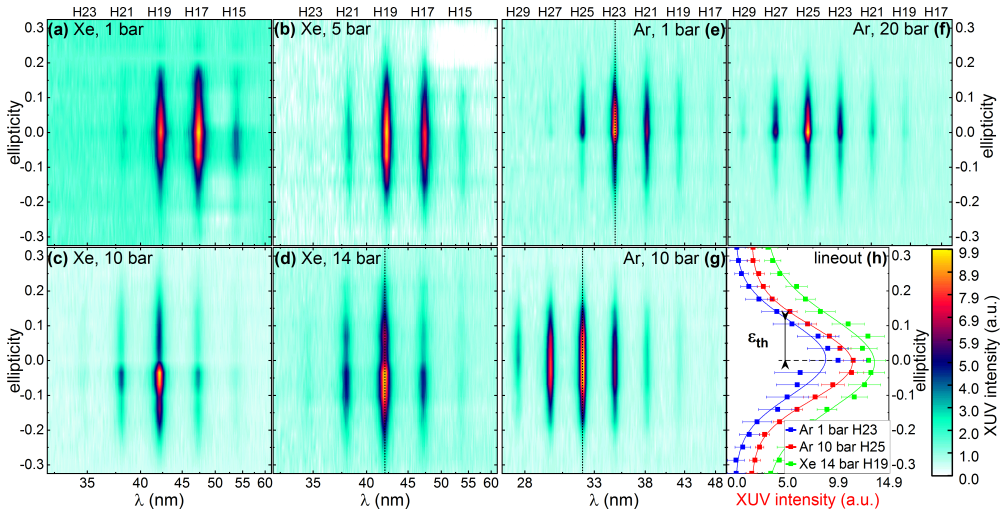

Figure 1. *HHG spectra as a function of the driver pulse ellipticity for different gases and backing pressures. Xe with (a) 1 bar, (b) 5 bar, (c) 10 bar and (d) 14 bar backing pressures; and Ar with (e) 1 bar, (g) 10 bar and (f) 20 bar backing pressures. The lineouts for Ar 1and 10 bar and Xe 14 bar are presented in (h), showing the evaluation method of threshold ellipticity, ε*th *to be used in Fig. 4. Threshold ellipticities in (h) are 0.12, 0.12 and 0.14, respectively. For better visibility, curves in (h) are offset by 1.5 units each.*

We also undertook the compilation of a major review article on strong-field nanooptics to appear in the leading review journal of physics, Reviews of Modern Physics.

Femtosecond photonics. — We studied the evolution of femtosecond breakdown in lithographically produced plasmonic nanoparticles with increasing laser intensity. Localized plasmons were generated with 40-fs laser pulses with up to 1.4×1012 W/cm2 peak intensity. The damage morphology shows substantial variation with intensity, starting with the detachment of hot spots and stochastic nanoparticle removal, ranging to precise nanolithographic mapping of near-field distributions via ablation. The common feature of these phenomena is the central role played by the single plasmonic hot spot of the triangular nanoparticles used. We also derive a damage threshold value from stochastic damage trends on the arrays fostering the optimization of novel nanoarchitectures for nonlinear plasmonics and plasmonically enhanced high harmonic generation .

Laser fusion enhanced by metal nanoparticles. — We also studied localized surface plasmon assisted laser fusion. Here, achieving the necessary high temperature for ignition could be realized not by compression, but by direct heating. This can be achieved by placing plasmonic nanorods or nanoshells into the ignition target. „Time-like" implosion of the total target volume may be realized by proper distribution of the nanoparticles in the target volume. Shorter (picosecond instead of nanosecond) laser pulses, smaller and flat samples and only 2 laser beams (hitting the target from opposite directions) may be used and a few times 10 Joule energy pulses may already lead to implosion .

2018

Strong-field interactions and nano-optics experiments. — Probing nanooptical near-fields is a major challenge in plasmonics. We demonstrated an experimental method based on utilizing ultrafast photoemission from plasmonic nanostructures that is capable of probing the maximum nanoplasmonic field enhancement in any metallic surface environment (Rácz et al., Nano Lett. 2017). Directly measured maximum field enhancement values for various samples are in good agreement with detailed finite-difference time-domain simulations. These results established ultrafast plasmonic photoelectrons as versatile probes for nanoplasmonic near-fields. We extended this method to probe the evolution of plasmonic near-fields on few-femtosecond time-scales, representing the natural time-scale of the buildup and decay of collective electron oscillations by light. Fig. 1 shows the scheme and results of these experiments.

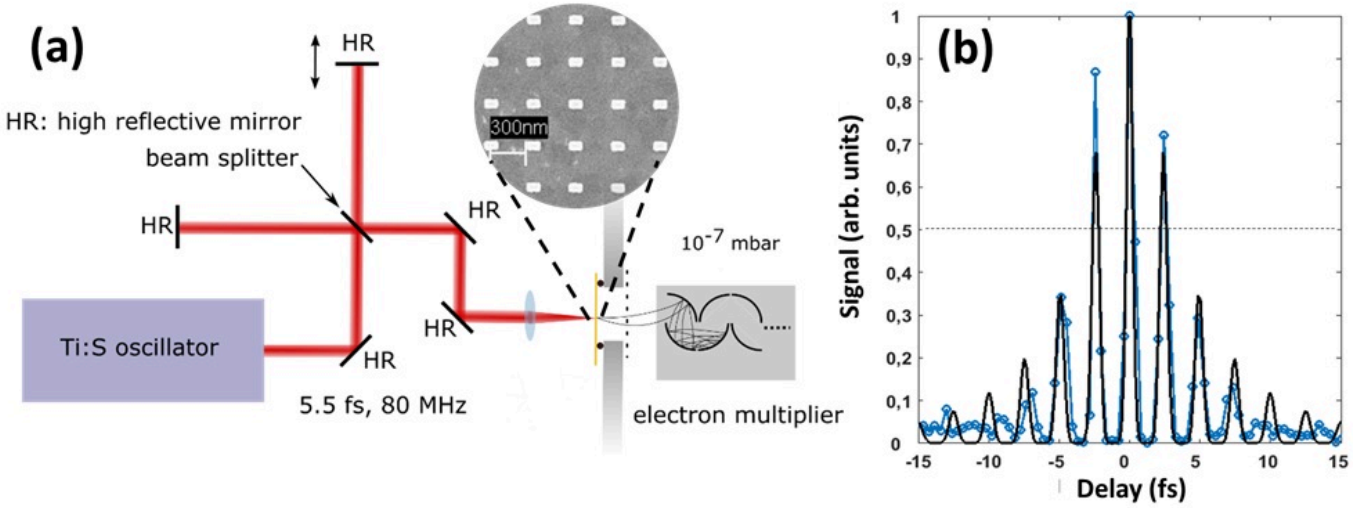

Figure 1. *(a) The output of an interferometric autocorrelator setup illuminated by 5.5-fs laser pulses is focused onto a substrate with plasmonic nanoparticles. Photoelectron spectra are recorded in vacuum. (b) Measured (blue) and reconstructed (black) third order interferometric autocorrelation curves of the few-femtosecond plasmonic near-field.*

In addition, we used this method to probe the coupling between propagating and localized surface plasmon modes, a fundamental question in plasmonics (Budai, Pápa et al., Nanoscale 2018).

Laser fusion enhanced by metal nanoparticles. — Localized surface plasmon assisted laser fusion was also studied (Kroó et al., Laser and Particle Beams 2018), where achieving the needed high temperature for ignition could be realized not by compression, but by direct heating. This can be achieved by putting into the target plasmonic nanorods or nanoshells. „Time-like" implosion of the total target volume may be realized by proper distribution of the nanoparticles in the target volume. Shorter (picosecond instead of nanosecond) laser pulses, smaller and flat samples and only 2 laser beams (hitting the target from opposite directions) may be used and a few times 10 Joule energy pulses may already lead to implosion.

Femtosecond photonics. — Improving the laser-induced damage threshold of optical components is a basic endeavor in femtosecond technology. By testing more than 30 different femtosecond mirrors with 42 fs laser pulses at 1 kHz repetition rate, we found that a combination of high-bandgap dielectric materials and improved design and coating techniques enable femtosecond multilayer damage thresholds exceeding 2 J/cm^2 in some cases. We also studied damage threshold dependence as a function of the number of interacting pulses and other relevant parameters.

Ultrashort laser pulses provide an excellent dry and clean patterning technique in nanoscience for preparing quantum dots and quantum wires as well as depositing nanocrystalline grains of technologically important semiconductors. We experimentally demonstrated the formation of silicon carbide (SiC) nanocrystals with wide size distribution (70–700 nm) by irradiation of carbon layers deposited on silicon wafers with ultrashort laser pulses of 42 fs pulse duration with 1 kHz repetition rate. Surface morphology of the laser irradiated region monitored by scanning electron microscopy (SEM) exhibits nanocrystalline agglomerates of various size in the vicinity of ablated craters. Transmission electron microscopy (TEM) measurements show the occurrence of ~ 100 nm size cubic and hexagonal SiC polytypes in addition to Si and amorphous silica nanoparticles. Further development of this laser-induced process and the accurate control of the laser pulse parameters can open new routes for preparing tailor-made SiC nanomaterials that have useful properties for electronic and biomedical applications.

2017

Strong-field interactions and nano-optics experiments. — Probing nanooptical near-fields is a major challenge in plasmonics. We demonstrated an experimental method based on utilizing ultrafast photoemission from plasmonic nanostructures that is capable of probing the maximum nanoplasmonic field enhancement in any metallic surface environment. Directly measured maximum field enhancement values for various samples are in good agreement with detailed finite-difference time-domain simulations. These results establish ultrafast plasmonic photoelectrons as versatile probes for nanoplasmonic near-fields. Figure 1 shows test samples and spectral cutoffs according to which maximum field enhancement values are determined.

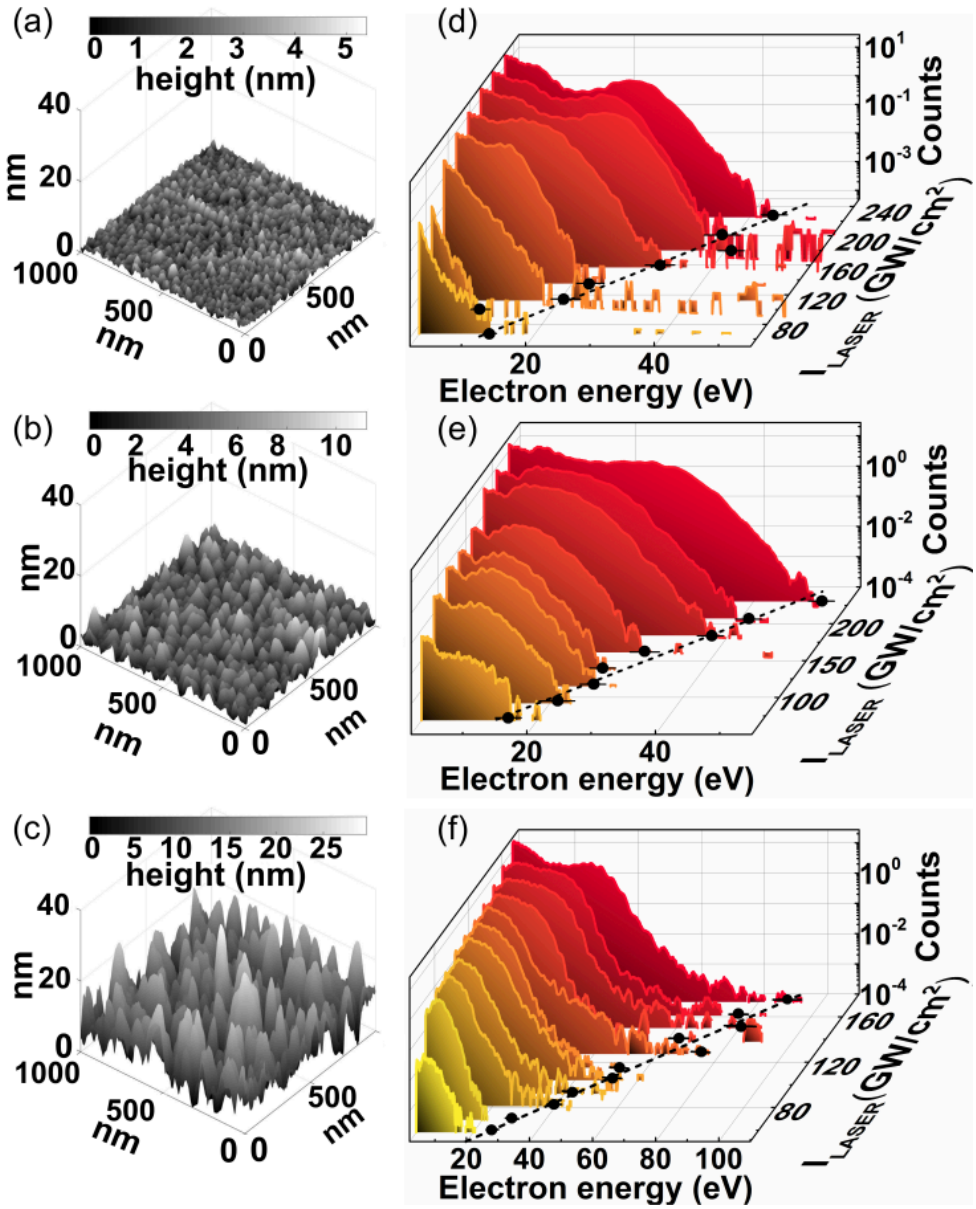

Figure 1. (a-c) *Atomic force microscope scans of plasmonic surfaces with controlled, different rms roughnesses of 0.8 nm, 1.6 nm and 4.5 nm, after applying a tip shape deconvolution procedure. (d-f) Plasmonic photoelectron spectra (logarithmic scale) from the three surfaces by generating plasmons with a 38-fs laser pulse with different focused intensities. Black symbols correspond to electron spectral cutoffs. Cutoff error bars are determined according to fit uncertainty.*

Surface plasmon experiments. — We studied electron emission induced by intense, femtosecond plasmon field on a periodically structured gold film. Results on previous, disordered samples agreed well qualitatively (see electron pairing at an intensity of around 80 GW/cm2), however, new phenomena were discovered as well. Most interestingly, we found narrow resonances in time-of-flight electron spectra that can be interpreted as a quantum interference effect. Emission related to electron pairs produce different narrow resonances of this kind.

Femtosecond photonics. — Improving the laser-induced damage threshold of optical components is a basic endeavor in femtosecond technology. By testing more than 30 different femtosecond mirrors with 42 fs laser pulses at 1 kHz repetition rate, we found that a combination of high-bandgap dielectric materials and improved design and coating techniques enable femtosecond multilayer damage thresholds exceeding 2 J/cm2 in some cases. We also studied damage threshold dependence as a function of the number of interacting pulses and other relevant parameters. A significant x2.5 improvement in damage resistance can also be achieved for hybrid Ag-multilayer mirrors exhibiting more than 1 J/cm2 threshold with a clear anticorrelation between damage resistance and peak field strength in the stack.

Theoretical research. — In studying the quantum phase properties of electromagnetic radiation fields, we have recently derived the regular-phase coherent states, which are in fact SU(1,1) coherent states, introduced earlier in a more general context. In the one-mode representation, these states are generated by a perturbed electromagnetic oscillator Hamiltonian containing an intensity-dependent coupling term. By applying this abstract formalism for a completely different system, we have discussed a new physical realization of these regular-phase coherent states, which may be relevant in the non-perturbative theory of some strong-field processes. We have shown that the motion of a charged particle in a Coulomb field can naturally be described by using SU(1,1) generators and a fictious time parameter, the so-called eccentric anomaly. By analysing the interaction of a Rydberg atom with a strong microwave field at the main resonance, we have described squeezing and stretching in real space as a result of the generation of SU(1,1) coherent states for the Coulomb problem. If the microwave field is linearly polarized along the *z*-direction, the Bargmann index of the sub-space of these states is (|*m*|+1)/2, where *m* is the (conserved) z-component of the angular momentum. In Figs. 2 and 3, we illustrate the resulting spatial distorsions of the wave functions, for two initial set of parabolic quantum numbers.

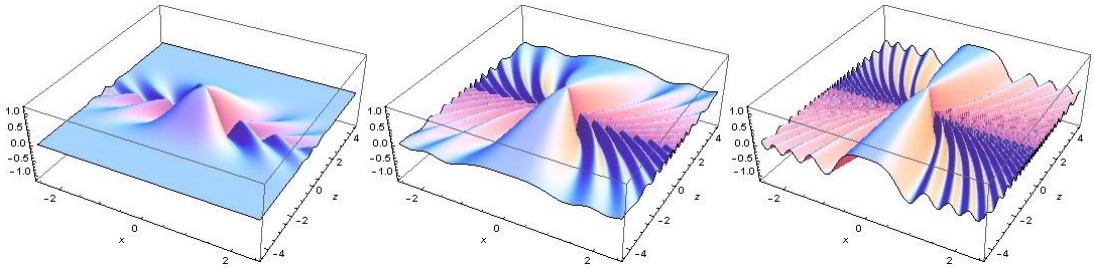

Figure 2. *The left figure (a) shows the initial wave function (with parabolic quantum numbers: m=0, n1=0, n2=60) as a function of the x and z coordinates. The microwave field is assumed to be linearly polarized along the z-direction. The central (b) and the right (c) figures display the the distorted wave functions (stretching along the polarization, after the microwave field has been switched on) at two instants: after one and two cycles of the scaled time parameter, respectively.*

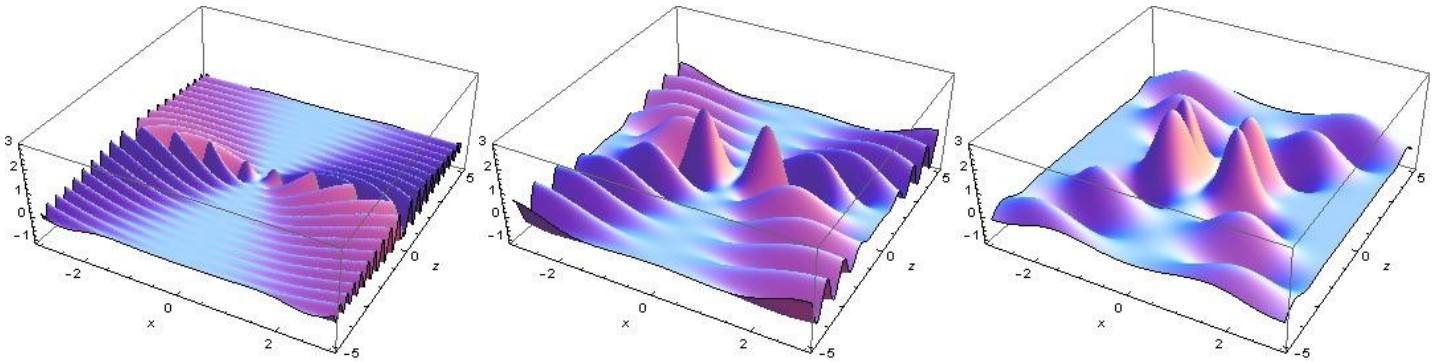

Figure 3. *The same as in Figure 2, but now with different intitial parabolic quantum numbers: m=1, n1=60, n2=0.*